First-principles study of the elastic and optical properties of the pseudocubic Si_3As_4, Ge_3As_4 and Sn_3As_4

2007 J. Phys.: Condens. Matter 19 496215

(http://iopscience.iop.org/0953-8984/19/49/496215)

IOP PUBLISHING JOURNAL OF PHYSICS: CONDENSED MATTER

J. Phys.: Condens. Matter **19** (2007) 496215 (10pp) doi:10.1088/0953-8984/19/49/496215

First-principles study of the elastic and optical properties of the pseudocubic Si_3As_4, Ge_3As_4 and Sn_3As_4

Jian-Ming Hu[1,2], Shu-Ping Huang[1], Zhi Xie[1], Hui Hu[1] and Wen-Dan Cheng[1,3]

[1] State Key Laboratory of Structural Chemistry, Fujian Institute of Research on the Structure of Matter, The Chinese Academy of Sciences, Fuzhou 350002, People's Republic of China
[2] Training Department, Command Academy of Fuzhou, The Chinese People's Armed Police Force, Fuzhou 350002, People's Republic of China

E-mail: cwd@fjirsm.ac.cn

Received 6 September 2007, in final form 25 October 2007
Published 15 November 2007
Online at stacks.iop.org/JPhysCM/19/496215

Abstract

The elastic and optical properties of Si_3As_4, Ge_3As_4 and Sn_3As_4 systems with pseudocubic structure have been investigated by first-principles calculations. Our calculated results show that these compounds are mechanically stable after evaluating the calculated elastic constants. The calculated band structures and densities of state show that the three arsenides are semiconductors with narrow indirect band gaps. Furthermore, the optical constants, such as the dielectric function, refractive index and energy loss function, are calculated and presented in the study.

(Some figures in this article are in colour only in the electronic version)

1. Introduction

Since the prediction of a low compressibility solid β-C_3N_4 by Liu and Cohen [1], the structure and electronic behavior of IV_3V_4 compounds has attracted great attention due to their important potential applications in technical and scientific fields. Among them, the group IV nitrides possess low compressibility and high hardness, comparable with corundum and silicon carbide used in cutting and grinding applications [1–7]. Meanwhile, first-principles theoretical studies [8–12] have predicted that the group IV nitrides are wide-band-gap semiconductors, whose electro-optic properties might be comparable with those of group III(B) nitrides (AlN/GaN/InN). For the group IV phosphides, first-principles theoretical studies predicted that the most stable phase is the pseudocubic (PC) structure (space group $P\bar{4}2m$, (111)) [13–17].

[3] Author to whom any correspondence should be addressed.

To explore their applications, the optical properties of the IV_3P_4 system with PC structure have been investigated using a first-principles theoretical approach [18].

Recently, the structural properties of IV_3As_4 polymorphs have also been investigated by using the first-principles calculations and successfully predicted that the most stable phase of those compounds is the PC structure [19]. However, there were a few reports on the theoretical studies of elastic constants and optical properties in the IV_3As_4 system, despite their important potential applications in the chemical and physical field. On the other hand, there is still a lack of experimental data for the crystalline IV_3As_4. Therefore, to understand the properties of IV_3As_4 polymorphs and explore their applications, further theoretical and computational studies on the structures, elastic constants, electronic and optical properties of IV_3As_4 would be necessary.

In this work, the structural parameters of the pseudocubic Si_3As_4, Ge_3As_4 and Sn_3As_4 will first be calculated by using the first-principles method based on plane waves and pseudopotentials. Next the elastic constants and electronic properties of the three arsenides will be discussed, and finally the optical properties of these compounds will be investigated in terms of the results calculated by the density functional theory (DFT).

2. Computational details

All calculations were carried out using the density functional theory, as implemented in the CASTEP code [20]. The interactions between the ions and the electrons were described using the norm-conserving pseudopotential [21], and the electron–electron interaction was treated within the gradient-corrected generalized gradient approximation (GGA) by the Perdew, Burke and Ernzerhof (PBE) exchange–correlation potential [22]. The structural parameters and mechanical properties were calculated until the energy, force, stress and self-consistent field (SCF) on each atom converged to 5.0×10^{-6} eV/atom, 0.01 eV Å^{-1}, 0.02 GPa and 5.0×10^{-7} eV/atom, respectively. The electronic wavefunctions are expanded in a plane wave basis set with periodic boundary conditions, and a plane wave energy cut-off of 800 eV was used for all structures. The numerical integration of the Brillouin zone (BZ) was performed using a $6 \times 6 \times 6$ Monkhorst–Pack k-point sampling procedure for structural optimization. For the electronic structure and linear optical calculations, a $16 \times 16 \times 16$ k mesh in the irreducible portion of the BZ and 36 empty bands were used.

The linear response of a system to an external electromagnetic field with a small wavevector is measured through the complex dielectric function $\varepsilon(\omega) = \varepsilon_1(\omega) + \mathrm{i}\varepsilon_2(\omega)$. The imaginary part of the dielectric function, $\varepsilon_2(\omega)$, is given by the equation [23]

$$\varepsilon_2^{ij}(\omega) = \frac{8\pi^2\hbar^2e^2}{m^2V}\sum_k\sum_{\mathrm{cv}}(f_\mathrm{c} - f_\mathrm{v})\frac{p_{\mathrm{cv}}^i(k)\,p_{\mathrm{vc}}^j(k)}{E_{\mathrm{vc}}^2}\delta[E_\mathrm{c}(k) - E_\mathrm{v}(k) - \hbar\omega], \tag{1}$$

where $\delta[E_\mathrm{c}(k) - E_\mathrm{v}(k) - \hbar\omega]$ denotes the energy difference between the conduction and valence bands at the k point with absorption of a quantum $\hbar\omega$. f_c and f_v represent the Fermi distribution functions of the conduction and valence bands. The term $p_{\mathrm{cv}}^i(k)$ denotes the momentum matrix element transition from the energy level c of the conduction band to the level v of the valence band at the k point in the Brillouin zones, and V is the volume of the unit cell. m, e and $\hbar$ are respectively the electron mass, charge and Planck's constant divided by 2π. The real parts of the dielectric functions $\varepsilon_1(\omega)$ can be derived from the imaginary parts of the dielectric functions $\varepsilon_2(\omega)$ by the Kramers–Krönig relations.

When the dielectric function is obtained, the other linear optical parameters, such as linear refractive index, absorption coefficient, reflectivity and electron energy loss (EEL) function, can be derived from it.

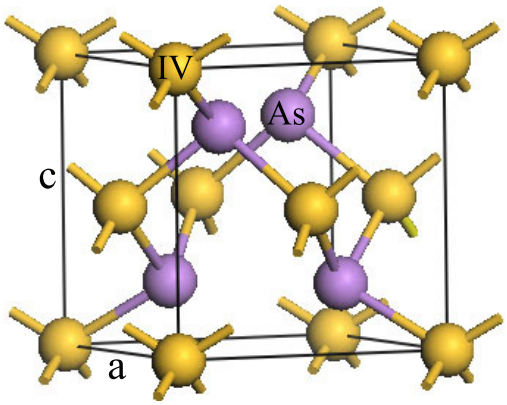

Figure 1. A ball–stick model of pseudocubic IV_3As_4 compounds.

Table 1. Calculated lattice parameters (a and c), fractional coordinates of As (u, v, w) (Note: the positions of group IV atoms are fixed by symmetry at (0, 0, 0) and (0.5, 0, 0.5) for these compounds, respectively), second-order elastic constants (C_{ij}), bulk modulus (B) and anisotropic Young's moduli (E) for all the compounds.

	Si_3As_4	Ge_3As_4	Sn_3As_4
a (Å)	5.2743, 5.357[a]	5.3270, 5.499[a]	5.7034, 5.848[a]
c (Å)	5.2755, 5.358[a]	5.3267, 5.518[a]	5.7051, 5.849[a]
(u, v, w)	(0.2762, 0.2762, 0.2238)	(0.2776, 0.2776, 0.2224)	(0.2822, 0.2822, 0.2178)
C_{11} (GPa)	108.39	100.68	70.47
C_{33} (GPa)	108.46	100.36	70.49
C_{44} (GPa)	57.88	51.61	38.32
C_{66} (GPa)	57.91	51.45	38.26
C_{12} (GPa)	41.09	37.86	31.34
C_{13} (GPa)	41.01	37.87	31.25
B (GPa)	63.49	58.77	44.35
$E_{x,y}$ (GPa)	85.84	79.95	51.21
E_z (GPa)	85.95	79.65	51.31

[a] Calculation, reference [19].

3. Results and discussion

Figure 1 illustrates a ball and stick diagram of the PC structures of IV_3As_4 compounds. The PC phase can be approximately considered as a defect zinc-blende structure, with one missing group IV atom at face center (top or bottom surface in figure 1). Table 1 lists the calculated lattice constants a and c and fractional coordinates of As (u, v, w) for the three group IV arsenides, and it shows that our results of the lattice constant agree well with previous theoretical results [19] within the difference of about 3.5% and there is no big difference between a and c. Therefore, these compounds show little anisotropic properties though atoms are missing on the planes of the ideal zinc-blende structure along the c-axis. Similar results are obtained for the pseudocubic IV_3P_4 system [13–18].

The fractional coordinates of As (u, v, w) in IV_3As_4 with the ideal zinc-blende structure are (0.25, 0.25, 0.25). However, the calculated fractional coordinates of As (u, v, w) in the three group IV arsenides are different from those of the ideal zinc-blende structures, indicating that the As atoms in these compounds are relaxed compared with those in the ideal zinc-blende structure.

To assess the mechanical stability of the three IV_3As_4 crystals, their elastic constants were calculated by using the finite strain techniques in the CASTEP package. According to Hooke's law, the linear elastic constants C_{ij} (giving the stress required to maintain a given strain) form a 6×6 symmetric matrix, having 27 different components, such that $\sigma_i = C_{ij}\epsilon_j$ for small stresses, σ, and strains, ϵ. Both stress and strain tensors have three tensile and three shear components. Any symmetrical structure may result in some components being equal and others zero. Thus, a tetragonal crystal has only six different symmetry elements ($C_{11} = C_{12}$, C_{12}, $C_{13} = C_{23}$, C_{33}, $C_{44} = C_{55}$ and C_{66}). Properties such as the bulk modulus B and shear modulus G (response to an isotropic compression), Young's modulus E etc may be computed from the values of C_{ij}.

In the present work, the elastic coefficients were determined from the first-principles method. This method usually involves setting either the stress or the strain to a finite value, re-optimizing any free parameters and calculating the other property (the strain or stress, respectively). Elastic coefficients can then be determined with a careful choice of the applied deformation. Generally, applying a given homogeneous deformation (strain) and calculating the resulting stress requires far less computational effort, since the unit cell is fixed and does not require optimization. This is the method implemented in CASTEP. Two strain patterns, one with non-zero first and fourth components, and another with non-zero third and sixth components, give stresses related to all six independent elastic constants for the tetragonal unit cell. Two positive and two negative amplitudes were used for each strain component with the maximum strain value of 0.3%, and then the elastic constants were determined from a linear fit of the calculated stress as a function of strain. The calculated elastic constants are shown in table 1.

The mechanical stability of a crystal requires the strain energy to be positive, which for a tetragonal crystal implies [24]

$$\begin{aligned} &C_{11} - C_{12} > 0, \qquad (C_{11} + C_{33} - 2C_{13}) > 0, \qquad C_{44} > 0, \\ &C_{66} > 0, \qquad (2C_{11} + C_{33} + 2C_{12} + 4C_{13}) > 0. \end{aligned} \tag{2}$$

From table 1, we can see that the three listed group IV arsenides are mechanically stable because their elastic constants satisfy equation (2), and do not display obvious anisotropy in elastic constants. For example, the longitudinal moduli, C_{11} (stiffness against {100}(100) uniaxial strain) and C_{33} (stiffness against {001}(001) uniaxial strain), indicate that C_{11} and C_{33} are the same within the accuracy of the theoretical method for Si_3As_4, with the c-axis (C_{33}) being about only 0.06% less than the a-axis (C_{11}). Of the most important characteristics, the shear moduli are much smaller than the coefficients related to uniaxial tensile or compression strain. For instance, C_{66} and C_{44} of Si_3As_4, which relate to resistance against {100}(010) and {010}(001) shear strain, respectively, yield only about 57.9 GPa.

The bulk modulus of a material, B, is a material property characterizing the compressibility of a material, which can be derived from the linear elastic constants C_{ij}. The calculated bulk modulus of the three group IV arsenides is also reported in table 1. It is noted that the value of bulk modulus decreases with increasing atomic number of the group IV atom. This can be seen by the fact that the value of bulk modulus decreases with increasing atomic number of the group IV atom.

The Young's moduli (E) are an important quantity for technological and engineering applications and provide a fundamental description of a material's mechanical behavior, which is defined as the ratio of the tensile stress in a material to the corresponding tensile strain. The calculated anisotropic Young's moduli of these compounds are also shown in table 1. The calculations also show that the Young's moduli of these compounds are slightly anisotropic.

Table 2. Calculated Voigt bulk modulus (B_V), Reuss bulk modulus (B_R), Voigt–Reuss–Hill averaged bulk modulus (B_{VRH}), Voigt shear modulus (G_V), Reuss shear modulus (G_R), Voigt–Reuss–Hill averaged shear modulus (G_{VRH}), band gap (E_g) and direct band gap at the Γ point (E_Γ) for all compounds.

	Si_3As_4	Ge_3As_4	Sn_3As_4
B_V (GPa)	63.50	58.77	44.35
B_R (GPa)	63.49	58.77	44.35
B_{VRH} (GPa)	63.50	58.77	44.35
G_V (GPa)	48.21	43.48	30.78
G_R (GPa)	44.97	40.99	27.70
G_{VRH} (GPa)	46.59	42.23	29.24
E_g (eV)	0.445, 0.42[a]	0.248, 0.16[a]	1.039, 0.39[a]
E_Γ (eV)	0.554	0.347	1.172

[a] Calculation, reference [19].

The shear modulus (G) is the most important parameter governing indentation hardness, depends on the nature of the bond and decreases as a function of ionicity, which is defined as the ratio of shearing stress to shearing strain within the proportional limit of a material. The hardness of a material is more correlated with the shear modulus than the bulk modulus [25]. As mentioned above, single crystals of group IV arsenides are currently unavailable and measurement of the individual elastic constants has not yet been reported. However, on the basis of the Voigt–Reuss–Hill approximation [26–28], the corresponding bulk and shear moduli from the single-crystal zero-pressure elastic constants have been calculated, which may be determined on the polycrystalline samples experimentally. The Voigt–Reuss–Hill averaged shear modulus G_{VRH} was obtained through the following equations: $G_{VRH} = (G_V + G_R)/2$, where the effective Voigt shear modulus G_V and Reuss shear modulus G_R for specific cases of tetragonal lattices are

$$G_V = \tfrac{1}{15}(2C_{11} + C_{33} - C_{12} - 2C_{13}) + \tfrac{1}{5}(2C_{44} + C_{66}), \tag{3}$$

and

$$G_R = \frac{15}{4(2s_{11} + s_{33}) - 4(s_{12} + 2s_{13}) + 3(2s_{44} + s_{66})}. \tag{4}$$

To compare with the bulk modulus of DFT calculation, the averaged Voigt–Reuss–Hill bulk modulus B_{VRH} was also obtained through the following equations: $B_{VRH} = (B_V + B_R)/2$, where the Voigt bulk modulus (B_V) and the Reuss bulk modulus (B_R) for specific cases of tetragonal lattices are

$$B_V = \tfrac{1}{9}(2C_{11} + C_{33}) + \tfrac{2}{9}(2C_{13} + C_{12}), \tag{5}$$

and

$$B_R = \frac{1}{(2s_{11} + s_{33}) + 2(2s_{13} + s_{12})}. \tag{6}$$

In equations (4) and (6), the s_{ij} are the elastic compliance constants, which describe the response of a material to an applied stress.

Using the above relations, the calculated B_V, B_R, B_{VRH}, G_V, G_R and G_{VRH} are given in table 2. From tables 1 and 2, the calculated Voigt bulk modulus (B_V), the Reuss bulk modulus (B_R) and the averaged Voigt–Reuss–Hill bulk modulus (B_{VRH}) are all equal to the computed bulk modulus B of DFT calculations for all compounds. The calculated averaged Voigt–Reuss–Hill shear moduli (G_{VRH}) of Si_3As_4, Ge_3As_4 and Sn_3As_4 are about 46.59, 42.23 and 29.24 GPa, respectively, indicating that the shear modulus decreases with the increasing atomic number of

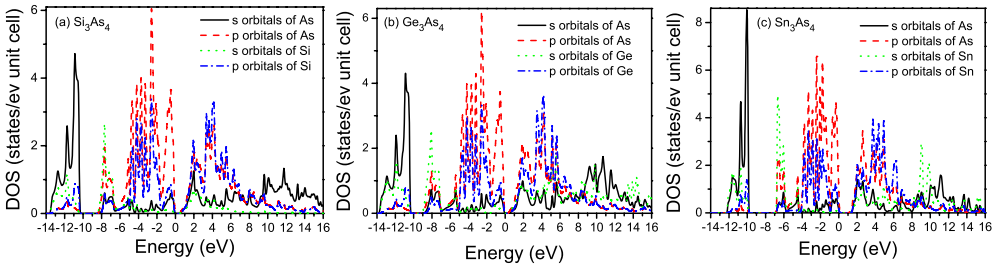

Figure 2. Calculated partial density of states of (a) Si_3As_4, (b) Ge_3As_4 and (c) Sn_3As_4 compounds, respectively.

group IV. In general, the value of shear moduli is an indication of the directional bonding between atoms. The degree of Cauchy violation ($C_{44}/C_{12} \neq 1$) indicates the deviation from a two-body central force model [7]; that is, the closer to one is the C_{44}/C_{12} ratio, the greater the ionic character between the two atoms. In this work, the group IV arsenides have $C_{44}/C_{12} = 1.41$ for Si_3As_4, 1.36 for Ge_3As_4 and 1.22 for Sn_3As_4. This indicates that bonding in Sn_3As_4 has more ionic character than the others.

To understand the mechanical properties of these three materials on a fundamental level, the partial densities of states (PDOSs) are calculated at zero pressure within the DFT method. The results are shown in figure 2. For Si_3As_4 (figure 1(a)), the main components of the PDOS at the bottom of the conduction band (CB) are the mixings of the Si and As valence orbitals. The states in the valence band (VB) between -14 and -10 eV are mainly composed of As(4s) states with a little contribution from Si(3s and 3p) states. At the peak of around -7.5 eV, the PDOS of Si_3As_4 clearly exhibits hybridizations between the 3s orbitals of Si and 4p valence orbitals of As. The strong hybridized states of Si(3p) and As(4p) between -6 and -1.5 eV are responsible for the covalent bonding of Si_3As_4. The states between -1.5 and 0 eV are mainly composed of As(4p) states with a little contribution from Si(3s and 3p) states. For Ge_3As_4 and Sn_3As_4, which contain more d orbitals than Si_3As_4, the atomic radii of Ge and Sn atoms are bigger than that of the Si atom, thereby decreasing the covalent bonding strength of such a compound. As a consequence, the bulk and shear moduli of Ge_3As_4 and Sn_3As_4 are lower than that of Si_3As_4. In view of the quantitative analysis from the overlap extent between the IV(np) and As(4p) states, as shown in figure 1, we find that the overlap extents between the Sn(5p) and As(4p) are the smallest among the overlap extents between the IV(np) and As(4p) states. For this reason, we can conclude that Sn_3As_4 has the most ionic character and smallest shear modulus and hardness in all the studied crystals.

As we know, the optical spectra are calculated from interband transitions. Then, we describe our calculated band structure. However, since the gross features of the band structure of the three compounds are very similar, we only present here the details of Si_3As_4 along many important directions on the BZ in figure 3. The first Brillouin zone of IV_3As_4 is also illustrated in figure 3. The corresponding energy gaps are given in table 2.

For these compounds, the upper VB edge is in the Γ–M direction and the lower CB edge is at the Γ point. For Si_3As_4, Ge_3As_4 and Sn_3As_4, it has a narrow indirect band gap of 0.445 eV, 0.164 eV and 1.039 eV, while the band gap at the Γ point is 0.554 eV, 0.488 eV and 1.172 eV, respectively. This shows that the differences between the indirect and direct band gaps of these compounds are small; the largest difference between the indirect and direct band gaps is 0.133 eV at the Γ point for Sn_3As_4. The calculated band gap of Sn_3As_4 is wider than the others. Our results are in agreement in the variation trend with those of Hu and Feng [19], although our

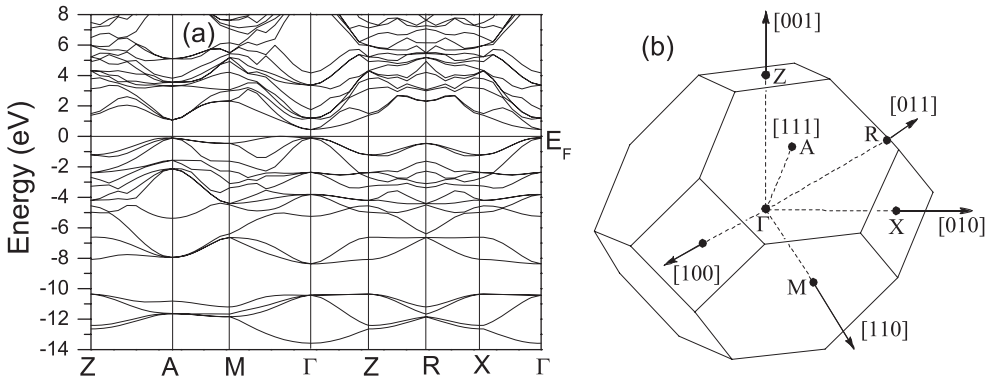

Figure 3. (a) The calculated band structure of the Si_3As_4 crystal and (b) the first Brillouin zone for pseudocubic IV_3As_4 compounds.

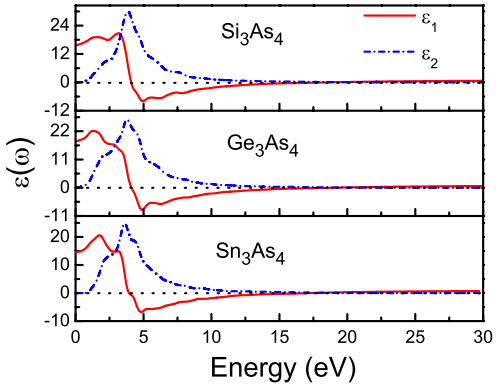

Figure 4. The calculated dielectric constants of the IV_3As_4 system.

gaps are larger. The differences may come from the parameters selected in previous calculations and ours. For example, we used the norm-conserving pseudopotentials, while the work of Hu and Feng [19] selected the ultrasoft pseudopotentials. However, since the DFT methods may underestimate the band gap and there is no experiment carried out for these compounds, the band gap calculated for example by GW quasiparticle theory [29], LDA + DMFT [30] and self-interaction-corrected DFT [31] may give a more accurate value. Anyway, the results show that all three compounds are indirect band gap semiconductors with narrow band gaps.

It is shown from the data of table 1 that the three arsenide crystals are not strongly anisotropic though they are structurally asymmetric, indicating that the difference between the longitudinal and transverse dielectric functions of the pseudocubic IV_3As_4 crystals is also small. We calculated both of the longitudinal and transverse dielectric functions to see that these two functions are almost identical within the difference of about 0.1%. Therefore, only the optical properties in polycrystalline structures are taken into consideration in this work for all crystals.

The dispersions of the imaginary parts $\varepsilon_2(\omega)$ of dielectric functions of polycrystalline phases are plotted in figure 4 for all structures, which can be used to describe optical absorption in crystals. It shows that each spectrum has a prominent absorption peak, with the main absorption peaks of Si_3As_4 at 3.84 eV as compared with the main peaks at 3.79 eV in Ge_3As_4

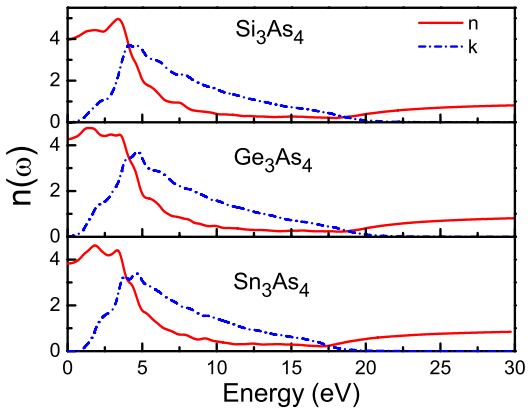

Figure 5. The calculated refractive index of IV_3As_4 compounds.

and 3.61 eV in Sn_3As_4. There is a systematic shift towards low energy from Si_3As_4 to Ge_3As_4 and to Sn_3As_4. Similar results are also found for the spinel cube γ-IV_3N_4 (IV = Si, Ge, Sn) by the Ching group [10] and for pseudocubic IV_3P_4 (IV = Si, Ge, Sn) by Xu [18]. The peak amplitude in Si_3As_4 is higher than in the other two crystals. From the calculated PDOS (see figure 1), it is clear that the prominent absorption peak of these compounds is mainly attributed to transitions from the As(4p) valence band to the group IV atom *n*p conduction band.

The real parts $\varepsilon_1(\omega)$ of dielectric functions of three compounds are also investigated. The zero-frequency limit of $\varepsilon_1(\omega)$ is the static dielectric constant $\varepsilon(0)$ of the electronic part, excluding any contribution from the lattice vibrations. The calculated static dielectric constants, $\varepsilon(0)$, are about 15.8287, 18.1690 and 14.6438 for Si_3As_4, Ge_3As_4 and Sn_3As_4, respectively, which are larger than those of the semiconductor Si, Ge and γ-IV_3N_4 [8–10]. According to the previous studies [8], a higher optical density for these compounds may have special applications in certain optical components. The calculated $\varepsilon(0)$ increases in the order of Sn_3As_4, Si_3As_4 and Ge_3As_4 for these crystals. A similar trend is also found for γ-IV_3N_4 (IV = Si, Ge, Sn) [8–10].

The $\varepsilon(0)$ of the Ge_3As_4 crystal has the largest value for these compounds, and a larger $\varepsilon(0)$ means a larger refractive index. The dispersion curves of refractive indices are plotted in figure 5; the refractive indices $n(0)$ of Si_3As_4, Ge_3As_4 and Sn_3As_4 are about 3.9785, 4.2625 and 3.8267, respectively, while the photon energy is zero.

The EEL function is an important parameter describing the energy loss of a fast electron traversing in the material, which can be evaluated from the dielectric function as $L(\omega) = \mathrm{Im}[-1/\varepsilon(\omega)] = \varepsilon_2(\omega)/[\varepsilon_1^2(\omega) + \varepsilon_2^2(\omega)]$. The peaks of loss function $L(\omega)$ represent the characteristic associated with the plasma resonance and the corresponding frequency is the so-called plasma frequency, ω_p. Above and below the plasma frequency the material will have the dielectric and metallic properties, respectively [32]. Figure 6 gives a plot of loss function $L(\omega)$ of these compounds. There is a broad peak for these compounds. The calculated peak of $L(\omega)$ of Si_3As_4 is located at about 18.82 eV, while those of Ge_3As_4 and Sn_3As_4 are shifted to lower energies at about 18.18 eV and 17.56 eV, respectively.

4. Conclusions

The mechanical and optical properties of the pseudocubic Si_3As_4, Ge_3As_4 and Sn_3As_4 were investigated using the *ab initio* pseudopotential density functional method. The energy band and density of states are calculated, and they show that the overlap extends between the IV

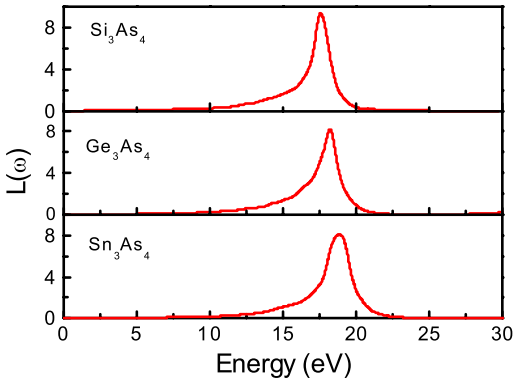

Figure 6. The calculated electron energy loss function of the IV_3As_4 system.

and As atom are decreasing in the order of Si $\geqslant$ Ge $>$ Sn. The findings indicate that the ionic bonding strength increases and crystal hardness decreases with the increase of atomic radius in IV group among IV_3As_4. The complex dielectric function, refractive index and energy loss function are also calculated based on the band structure. The results show that these compounds may have important potential applications in the optical absorption due to a small difference between the indirect and direct band gaps, and a high optical density.

Acknowledgments

The authors are grateful to the National Science Foundation of China (No 20373073), the National Basic Research Program of China (No 2007CB815307) and the Fund of Fujian Key Laboratory of Nanomaterials (No 2006L2005) for financial support.

References

[1] Liu A Y and Cohen M L 1989 *Science* **245** 1989
Liu A Y and Cohen M L 1990 *Phys. Rev.* B **41** 10727
[2] Zerr A, Miege G, Serghiou G, Schwarz M, Kroke E, Riedel R, Fuess H, Kroll R and Boehler R 1999 *Nature* **400** 340
[3] Leinenweber K, O'Keeffe M, Somayazulu M, Hubert H, McMillan P F and Wolf G W 1999 *Chem. Eur. J.* **5** 3076
[4] Sekine T, He H, Kobayashi T, Zhang M and Xu F 2000 *Appl. Phys. Lett.* **76** 3706
[5] Soignard E and McMillan P F 2004 *Chem. Mater.* **16** 3533
Soignard E, McMillan P F and Leinenweber K 2004 *Chem. Mater.* **16** 5344
[6] He J L, Guo L C, Yu D L, Liu R P, Tian Y J and Wang H T 2004 *Appl. Phys. Lett.* **85** 5571
[7] Soignard E, Somayazulu M, Dong J, Sankey O F and McMillan P F 2001 *J. Phys.: Condens. Matter* **13** 557
[8] Mo S D, Ouyang L, Ching W Y, Tanaka I, Koyama Y and Riedel R 1999 *Phys. Rev. Lett.* **83** 5046
[9] Ching W Y, Mo S-D and Ouyang L 2001 *Phys. Rev.* B **63** 245110
[10] Ching W Y and Rulis P 2006 *Phys. Rev.* B **73** 045202
[11] Dong J, Deslippe J, Sankey O F, Soignard E and McMillan P F 2003 *Phys. Rev.* B **67** 094104
[12] Hu J M, Cheng W D, Huang S P, Wu D S and Xie Z 2006 *Appl. Phys. Lett.* **89** 261117
[13] Lim A T L, Zheng J C and Feng Y P 2002 *Int. J. Mod. Phys.* B **16** 1101
[14] Lim A T L, Feng Y P and Zheng J C 2003 *Mater. Sci. Eng.* B **99** 527
[15] Huang M and Feng Y P 2004 *Comput. Mater. Sci.* **30** 371
[16] Huang M, Feng Y P, Lim A T L and Zheng J C 2004 *Phys. Rev.* B **69** 054112
[17] Huang M and Feng Y P 2004 *Phys. Rev.* B **70** 184116
[18] Xu M, Wang S, Yin G and Chen L 2006 *Opt. Express* **14** 711
[19] Hu C and Feng Y P 2006 *Phys. Rev.* B **74** 104102

[20] Segall M D, Lindan P J D, Probert M J, Pickard C J, Hasnip P J, Clark S J and Payne M C 2002 *J. Phys.: Condens. Matter* **14** 2717
[21] Lin J S, Qteish A, Payne M C and Heine V 1993 *Phys. Rev.* B **47** 4174
[22] Perdew J P, Burke K and Ernzerhof M 1996 *Phys. Rev. Lett.* **77** 3865
[23] Bassani F and Parravicini G P 1964 *Electronic States and Optical Transitions in Solid* (Cambridge: Cambridge University Press) p 129
[24] Wallace D C 1972 *Thermodynamics of Crystals* (New York: Wiley) chapter 1
[25] Teter D M 1998 *MRS Bull.* **23** 22
[26] Voigt W 1928 *Lehrbuch der Kristallphysik* (Leipzig: Teubner)
[27] Reuss A 1929 *Z. Angew. Math. Mech.* **9** 55
[28] Hill R 1952 *Proc. Phys. Soc. Lond.* **65** 350
[29] Hybertsen M S and Louie S G 1986 *Phys. Rev.* B **34** 5390
[30] Heaton R A, Harrison J G and Lin C C 1983 *Phys. Rev.* B **28** 5992
[31] Richter M 1998 *J. Phys. D: Appl. Phys.* **13** 1017
[32] Sun J, Zhou X-F, Fan Y-X, Chen J, Wang H-T, Guo X, He J and Tian Y J 2006 *Phys. Rev.* B **73** 045108